The Fayalite Content of Chondritic Olivine: Obstacle to Understanding the Condensation of Rocky Material

A. V. Fedkin
University of Chicago

L. Grossman
University of Chicago

Solar gas is too reducing for the equilibrium X_{Fa} in condensate olivine to reach the minimum X_{Fa} of the precursors of chondrules in unequilibrated ordinary chondrites (UOCs), 0.145, at temperatures above those where Fe-Mg interdiffusion in olivine stops. Vaporization of a region enriched in dust relative to gas compared to solar composition yields higher f_{O_2}, and condensate grains with higher equilibrium X_{Fa}, than in a solar gas at the same temperature. Only dust enrichment factors near the maximum produced in coagulation and settling models, together with C1 chondrite dust whose O content has been enhanced by admixture of water ice, can yield olivine condensate grains with radii ≥1 μm whose mean X_{Fa} exceeds the minimum X_{Fa} of the precursors of UOC chondrules over the entire range of nebular midplane cooling rates. This unlikely set of circumstances cannot be considered a robust solution to the problem of the relatively high fayalite content of UOC olivine.

1. INTRODUCTION

1.1. Minimum Fayalite Content of Chondrule Precursors in Unequilibrated Ordinary Chondrites

Olivine in primitive solar system matter contains significant amounts of fayalite. The mean mole fraction of fayalite, X_{Fa}, in olivine is 0.05–0.10 in CI and CM chondrites, ~0.07 in chondrules of CV chondrites, 0.38 in R chondrites, ~0.50 in the matrices of CO and CV chondrites (*Brearley and Jones,* 1998), and ~0.10 in interplanetary dust particles (*Rietmeijer,* 1998). *Huss et al*. (1981) showed that the mean X_{Fa} of submicrometer olivine grains in the opaque matrix of a given type 3 unequilibrated ordinary chondrite (UOC) is systematically higher than that of the larger olivine grains inside chondrules in the same meteorite. *Alexander et al*. (1989) suggested that the matrix olivine grains may have formed during parent-body metamorphic processes under relatively oxidizing conditions. Within the type 3 UOCs, *McCoy et al*. (1991) noted a progressive increase in mean X_{Fa} of olivine grains inside chondrules with increasing metamorphic grade, and attributed this to reactions between phases in chondrules and matrices during metamorphism. Consequently, in UOCs, the largest olivine grains in the least-metamorphosed types 3.0 and 3.1 are the ones whose compositions most likely reflect premetamorphic conditions. *Dodd et al*. (1967) obtained ~100 electron microprobe analyses of randomly selected, relatively large olivine grains, probably mostly in chondrules, in each of 31 ordinary chondrites. For the purpose of the present work, the mean X_{Fa} of olivine in each of Bishunpur, Krymka, and Semarkona from that study was averaged together with the mean X_{Fa} of chondrule olivine for the same meteorites from the study of *Huss et al*. (1981). The average X_{Fa} so obtained, 0.145, is only a lower limit to the mean X_{Fa} of olivine in chondrule precursors, as such materials are known to have undergone reduction to varying and generally unknown degrees during chondrule formation (*Rambaldi,* 1981). Regardless of the precise value of the characteristic X_{Fa} of the prechondrule, nebular material of these meteorites, it will be clear from what follows that its lower limit is much higher than can be produced during condensation of a solar gas.

1.2. Dust-enriched Systems

While thermodynamic treatments of condensation from a gas of solar composition have been enormously successful at explaining the mineralogy of such chondritic assemblages as Ca-, Al-rich inclusions (CAIs) (*Grossman,* 1980), it is also clear that these models are unable to account for all the mineralogical features of chondrites, including even these high-temperature objects (*MacPherson et al.,* 1983). Nowhere is this failure more evident than in the case of the fayalite content of olivine, the most abundant phase in ordinary chondrites. Equilibrium thermodynamic calculations predict that metallic Fe is at or near stability when olivine first condenses from a gas of solar composition at high temperature. As a result, X_{Fa} is initially nearly zero, and rises with falling temperature as metallic Fe is gradually oxidized (*Grossman,* 1972). A solar gas is so reducing, however, that

X_{Fa} is predicted to reach the levels found in UOCs only below 600 K, where Fe-Mg interdiffusion rates in olivine are negligible, preventing X_{Fa} from reaching these levels and leaving the problem of how chondrites obtained their FeO contents unsolved. This situation was reviewed thoroughly by *Palme and Fegley* (1990). They concluded that chondritic olivine with non-negligible X_{Fa} formed at higher temperature, and thus from a nebular region more oxidized than a solar gas, presumably due to enrichment in dust prior to its vaporization. Indeed, *Dohmen et al*. (1998) observed rapid uptake of FeO by forsterite in contact with metallic Fe under relatively oxidizing conditions at 1573 K.

Wood (1967) was the first to recognize that enrichment of dust in parts of the nebula, followed by its vaporization, could lead to regions having higher f_{O_2} than a gas of solar composition. The dust could either be presolar, having condensed in circumstellar envelopes prior to formation of the solar nebula, or could have condensed in cooler regions of the solar nebula and been transported to the location where ordinary chondrites were about to condense. Because the final product of condensation of such a dust-enriched region must still be chondritic in composition, however, the dust cannot have random composition but must be constrained to have chondritic proportions of condensable elements. If all the rock-forming elements were present as dust, a much greater proportion of the total O compared to the total C or H would be present in the dust, with the exact fractions depending on the precise composition of the dust. If, for example, the dust were of ordinary chondrite composition, it would contain ~27% of the total O, ~0.4% of the C, and ~3 ppm of the H. If it were of C1 chondrite composition, it would contain ~55% of the O, ~11% of the C, and ~190 ppm of the H. If, before nebular temperatures reached their maxima, such dust concentrated in certain regions relative to the gas compared to solar composition, then total vaporization of those regions would have produced a gas richer in O relative to H and C, and thus of higher f_{O_2}, than a solar gas. In an effort to avoid completely the problem of diffusing Fe^{2+} into previously formed forsterite crystals, *Ebel and Grossman* (2000) investigated the extreme conditions under which significant amounts of fayalite are stable in olivine at the very high temperatures at which the olivine first begins to condense. Under such conditions, Fe^{2+} is incorporated into the structure of the olivine crystals while they grow from the vapor. Because the dust enrichment factors required to produce those conditions are so unrealistically large, a different question is asked in the present paper. At the temperatures where fayalite is stabilized at the largest dust enrichment factors predicted by solar nebular coagulation and settling models, what is the maximum grain size that would allow diffusion to increase the X_{Fa} of previously condensed forsterite crystals to the minimum level of the nebular precursors of UOC chondrules?

Over the years, understanding the relatively high fayalite content of chondritic olivine has become even more difficult due to additional data on solar abundances of C and O (*Allende Prieto et al.,* 2001, 2002), which make the nebula more reducing; Fe-Mg interdiffusion rates in olivine (*Chakraborty,* 1997), which make diffusion slower; and non-ideality in olivine solid solutions, lowering the solubility of Fa in it (*Sack and Ghiorso,* 1989). In this paper, full condensation calculations are used to compute the equilibrium distribution of Fe as a function of temperature in a system of solar composition and in more oxidizing systems. These data are then combined with diffusion coefficients to estimate the mean X_{Fa} of condensate olivine grains of various sizes at the temperature at which diffusion stops, with a view toward understanding the formation conditions of the precursors of chondrules in the least-equilibrated ordinary chondrites. Preliminary versions of this work appeared in *Grossman and Fedkin* (2003) and *Fedkin and Grossman* (2004).

2. TECHNIQUE

2.1. Condensation Calculations

The computer program used by *Ebel and Grossman* (2000) employs the most up-to-date and mutually compatible thermodynamic dataset ever used in solar nebular condensation calculations. The numerical procedure used in that program fails at the relatively low temperatures of interest in the present work, however, due to the fact that gas-phase concentrations of refractory elements become vanishingly small. As a result, the immediate predecessor of that program, the one used by *Yoneda and Grossman* (1995), was used herein. It has the additional advantage of being able to compute the complete condensation sequence at 1° temperature intervals from 2000 to 500 K in minutes on a Pentium 4-based PC, whereas the *Ebel and Grossman* (2000) program requires many days on an SGI Origin 2000 with an R10000 processor. For high-temperature condensation of a gas of solar composition, results of both programs are compared and discussed by *Ebel and Grossman* (2000).

In this work, the same thermodynamic data were used as in *Yoneda and Grossman* (1995), with the following exceptions. Errors in the *Chase et al.* (1985) data for gaseous C_2N_2, C_2H_2, CN, and HS were corrected as in *Ebel and Grossman* (2000), and an error was corrected in the *Chase et al*. (1985) tables for another species, $S_2O_{(g)}$. Data for troilite, FeS, were taken from *Gronvold and Stolen* (1992), instead of from *Robie et al*. (1978). Data for olivine and orthopyroxene end members were taken from *Berman* (1988), instead of from *Robinson et al*. (1982). While *Yoneda and Grossman* (1995) treated olivine and orthopyroxene as ideal solutions, they were modeled as non-ideal, regular solutions in the present work, as in *Sack and Ghiorso* (1989). For olivine, the solution parameter for the excess free energy of mixing was taken directly from that work, and, for orthopyroxene, we used from that work the equivalent solution parameter in the absence of ordering at its reference pressure. For calibration of the solution mod-

els for olivine and orthopyroxene, *Sack and Ghiorso* (1989) used distribution coefficients for the Fe-Mg exchange reaction between them. These were taken from natural and synthetic assemblages, most of which equilibrated in the temperature range 873 to 1273 K, thus bracketing the temperature range of interest in this work.

As in *Yoneda and Grossman* (1995), the *Anders and Grevesse* (1989) estimates of the relative atomic abundances of the elements in the solar system were used, except for that of S, which was taken from the compilation of *Lodders* (2003), and for those of O and C, which were taken from new solar photospheric determinations by *Allende Prieto et al*. (2001) and (2002), respectively. Using *Lodders*' (2003) average S concentration in C1 chondrites of 5.41 wt%, instead of the 6.25 wt% used by *Anders and Grevesse* (1989), reduces the solar system abundance of S by 13.4%, to 4.46×10^5 atoms per 10^6 Si atoms. Compared to the data of *Anders and Grevesse* (1989), the new O and C abundances of 1.37×10^7 and 6.85×10^6 relative to Si = 1×10^6 are 42% and 32% lower, respectively, and yield a slightly higher C/O ratio, 0.50 compared to 0.42.

2.2. Diffusion Calculations

The dependence of the Fe-Mg interdiffusion rate in olivine on temperature, f_{O_2}, olivine composition, and crystallographic direction has been the subject of several experimental studies. *Miyamoto et al*. (2002) corrected the bulk interdiffusion coefficients of *Nakamura and Schmalzried* (1984) as well as the c-axis data from the work of *Buening and Buseck* (1973), *Misener* (1974), and *Chakraborty* (1997) to a constant X_{Fa}(= 0.14) and f_{O_2}(= 10^{-12}), and plotted the logarithms of these corrected interdiffusion coefficients, D, vs. 1/T. On this plot, the data from these four studies lie along four subparallel straight lines offset from one another by a total range of more than 2 orders of magnitude parallel to the log D axis. Strictly speaking, because *Nakamura and Schmalzried* (1984) measured bulk interdiffusion coefficients, their data must be resolved into interdiffusion coefficients parallel to each crystallographic axis in order to compare them with data from the other studies. Although the degree of anisotropy differs, both *Buening and Buseck* (1973) and *Misener* (1974) found that the interdiffusion rates parallel to the c-axis are higher than those parallel to the a-axis, which are greater than those parallel to the b-axis. Using the anisotropies of *Misener* (1974), a geometric correction was made to the bulk interdiffusion coefficients of *Nakamura and Schmalzried* (1984) in order to estimate the interdiffusion coefficient parallel to the c-axis consistent with the latter data. This calculation results in a D parallel to the c-axis, which is approximately twice the bulk D of *Nakamura and Schmalzried* (1984).

Comparing only c-axis data, the largest values of D come from the work of *Buening and Buseck* (1973) and the lowest from *Chakraborty* (1997). At 1323 K, the D of *Misener* (1974) is a factor of ~14 higher, and that of *Nakamura and Schmalzried* (1984) a factor of ~10 higher, than the value of *Chakraborty* (1997). As discussed by *Chakraborty* (1997), poor f_{O_2} control may have affected the *Misener* (1974) data, and use of polycrystalline materials may have compromised the work of *Buening and Buseck* (1973) and *Nakamura and Schmalzried* (1984). Accordingly, the *Chakraborty* (1997) data were employed in this study, by using all his data points with <20% error in a regression of their logarithms against 1/T and X_{Fa}. Because all of *Chakraborty*'s (1997) measurements were at one f_{O_2}, the same dependence of log D on log f_{O_2} was adopted as in *Buening and Buseck* (1973) and *Nakamura and Schmalzried* (1984). The resulting expression for diffusion along the c-axis is

$$\log D = -6.511 + (1/6)\log f_{O_2} - 12092.0/T + 3.351X_{Fa} \quad (1)$$

According to *Tscharnuter and Boss* (1993), the midplane of a dust-enshrouded solar nebular disk experiencing a declining mass accretion rate cools from 1500 K to very low temperature in ~10^5–10^6 yr. If this global cooling occurs at a rate proportional to temperature, the temperature falls exponentially with time at decay constants of 4.32×10^{-5} and 4.32×10^{-6} yr^{-1} for these respective cooling times, hereinafter referred to as "fast" and "slow" cooling respectively. At these rates, the time required to cool from 1200 to 800 K, for example, is ~9×10^3 yr in the fast cooling case and ~9×10^4 yr for slow cooling. For each decay constant, the cooling rate of the solar nebula was calculated at 10^{-6} K temperature intervals and, from these, the cooling time was computed for all intervals.

A finite-difference technique was used to solve the diffusion equation for spherical geometry (*Crank,* 1975) with both a diffusion coefficient and surface X_{Fa} that vary with time, assuming that the surface of the olivine condensate crystal equilibrates with the nebular gas instantaneously. For calculation of the fayalite concentration profile, the grain was assumed to consist of 145 shells of equal thickness from core to rim. The mole fraction fayalite was assumed to be zero in each shell as an initial condition. In all cases investigated in this work, an initial temperature below the condensation temperature of olivine was selected such that, upon cooling, diffusion caused the fayalite concentration throughout the interior of the grain to rise to the level of the surface concentration, producing a uniform profile at some lower temperature. For the first temperature step, the c-axis interdiffusion coefficient was calculated from equation (1), using the f_{O_2} corresponding to the initial temperature taken from a condensation calculation for the appropriate system composition. The surface X_{Fa} and f_{O_2} were calculated by the condensation program at 1 K intervals. Each temperature step was further subdivided into 10^6 equal steps, at which the f_{O_2} and equilibrium X_{Fa} were interpolated. The interdiffusion coefficient in each shell of the next temperature step was calculated from the interpolated temperature and f_{O_2}, and the radial variation of X_{Fa} in the previous step. Because the time taken for the nebula to cool through each 10^{-6} K temperature interval is known, the

interdiffusion coefficient and equilibrium X_{Fa} are also known as a function of time for each of the slow and fast cooling cases.

3. RESULTS AND DISCUSSION

3.1. Solar Gas

Although it is commonly assumed that the P_{H_2O}/P_{H_2} ratio is constant for a system of solar composition, it actually varies continuously with temperature, as does the oxygen fugacity, f_{O_2}. Shown in Fig. 1 is the variation with temperature of $\log f_{O_2}$ of the gas in equilibrium with condensates in a system of solar composition at a total pressure, P^{tot}, of 10^{-3} bar over the range of temperatures relevant to high-temperature condensation. Shown for comparison is the curve for equilibrium between iron and wüstite, $Fe_{0.947}O$. Above the latter curve, pure metallic Fe is unstable; below it, pure FeO is unstable. While $\log f_{O_2}$ of a solar gas varies from –15.3 at 1800 K to –19.6 at 1400 K, the $\log f_{O_2}$ for iron-wüstite (IW) equilibrium also falls over this temperature interval, and by almost the same amount. Thus, over this temperature interval, the f_{O_2} of a solar gas remains 6.6 to 6.7 log units more reducing than that necessary to equilibrate iron and wüstite, and its $\log f_{O_2}$ is abbreviated as IW-6.6.

Also shown in Fig. 1 is the curve for $\log f_{O_2}$ of a gas that is solar in composition except that its C, O, and S abundances are those of *Anders and Grevesse* (1989). Note that it is ~0.7 log units more oxidizing than the current solar gas curve over this temperature interval. This is due to the well-known effect of $CO_{(g)}$ (*Larimer,* 1975). This molecule is so stable in cosmic gases that it consumes the entirety of whichever of C and O is the lower in abundance, leaving the excess of the more-abundant element to form other molecules and condensates. The lower C/O ratio of *Anders and Grevesse* (1989) leaves a greater fraction of the O available to form the next most abundant O-containing species, $H_2O_{(g)}$. Coupled with the greater O/H ratio of the *Anders and Grevesse* abundance table, this leads to a higher P_{H_2O}/P_{H_2} ratio and thus a higher f_{O_2} than given by the abundances adopted herein.

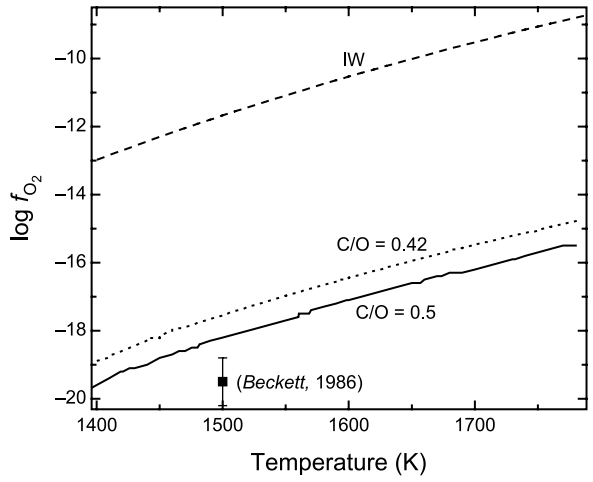

Fig. 1. Variation of the logarithm of the oxygen fugacity with temperature in equilibrium with condensates in a system of solar composition at a total pressure of 10^{-3} bar for C/O ratios of 0.42 (*Anders and Grevesse,* 1989) and the value used in this work, 0.50 (*Allende Prieto et al.,* 2001, 2002), compared to that of the iron-wüstite (IW) buffer. Also shown is the solar nebular oxygen fugacity at 1500 K, estimated from Allende refractory inclusions by *Beckett* (1986).

An independent estimate of the f_{O_2} of solar gas comes from the mineralogy of type B refractory inclusions in C3 chondrites. These objects are widely regarded as having condensed, melted, and recrystallized in a gas of solar composition (*Grossman et al.,* 2000, 2002). A major phase in all such inclusions is fassaite (*Dowty and Clark,* 1973), a Ca-,Al-rich clinopyroxene containing several weight percent of Ti, one-third to two-thirds of which is Ti^{3+} and the remainder Ti^{4+}. This may be the only pyroxene known to contain trivalent Ti and, if so, formed under lower f_{O_2} than all other Ti-bearing pyroxenes in terrestrial and lunar rocks. *Beckett* (1986) crystallized pyroxenes of these compositions from melts having the compositions of type B inclusions at controlled temperature and f_{O_2}. From these experiments, he was able to calculate equilibrium constants at 1500 K for redox reactions involving Ti^{3+}-bearing and Ti^{4+}-bearing pyroxene components, $O_{2(g)}$, and coexisting spinel, anorthite, and melilite. Because fassaite crystallizes from these melts at the solidus, 1500 K, he was able to use these equilibrium constants together with analyses of coexisting phases in actual type B inclusions to calculate the f_{O_2} at which the fassaite formed. The average $\log f_{O_2}$ so calculated, –19.5 ± 0.7, is the sole data point plotted on Fig. 1. Although it lies closer to the f_{O_2} curve for the current C/O ratio than to the one for the *Anders and Grevesse* (1989) ratio, the upper end of its error bar still lies 0.6 log units below the current solar gas curve.

Regardless of whether the actual solar nebular f_{O_2} was that of a system whose C/O ratio was 0.42, 0.50, or even slightly higher than this, Fig. 1 shows why the degree of oxidation of Fe in primitive solar system materials is so difficult to understand. In the high-temperature interval where reaction kinetics are most favorable, the f_{O_2} of a gas of solar composition lies so far below IW that only vanishingly small concentrations of FeO would be expected in silicates that equilibrate with the major Fe-containing high-temperature condensate, metallic Ni-Fe.

In the temperature range considered in Fig. 1, virtually all the C in a system of solar composition is present as $CO_{(g)}$. Upon cooling at equilibrium, a temperature is reached below which a significant fraction of the $CO_{(g)}$ begins to form $CH_{4\,(g)}$ via the reaction,

$$CO_{(g)} + 3H_{2(g)} \leftrightarrow CH_{4(g)} + H_2O_{(g)} \qquad (2)$$

which also increases the P_{H_2O}/P_{H_2} ratio, making the system more oxidizing. In reality, however, reaction (2) is very

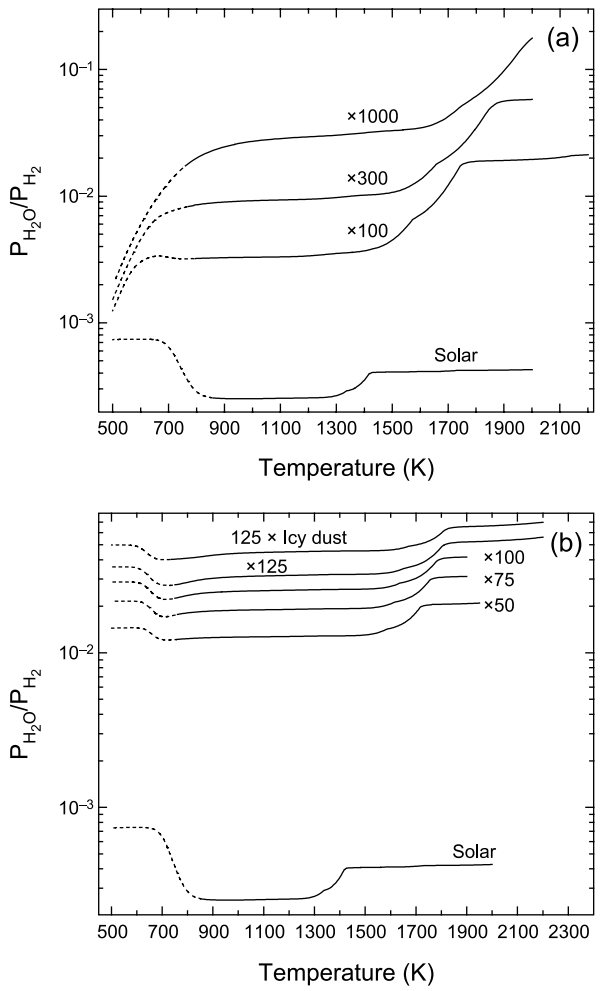

Fig. 2. Variation of the equilibrium P_{H_2O}/P_{H_2} ratio with temperature at $P^{tot} = 10^{-3}$ bar in systems enriched in **(a)** OC dust by factors of 100, 300, and 10^3 and **(b)** C1 dust by factors of 50, 75, 100, and 125 or in icy dust (see text) by a factor of 125 relative to solar composition, in all cases compared to that of a system of solar composition. Each curve is dashed below the temperature at which the P_{CH_4}/P_{CO} ratio becomes ≥0.01, where the P_{H_2O}/P_{H_2} ratio becomes significantly affected by reaction (2).

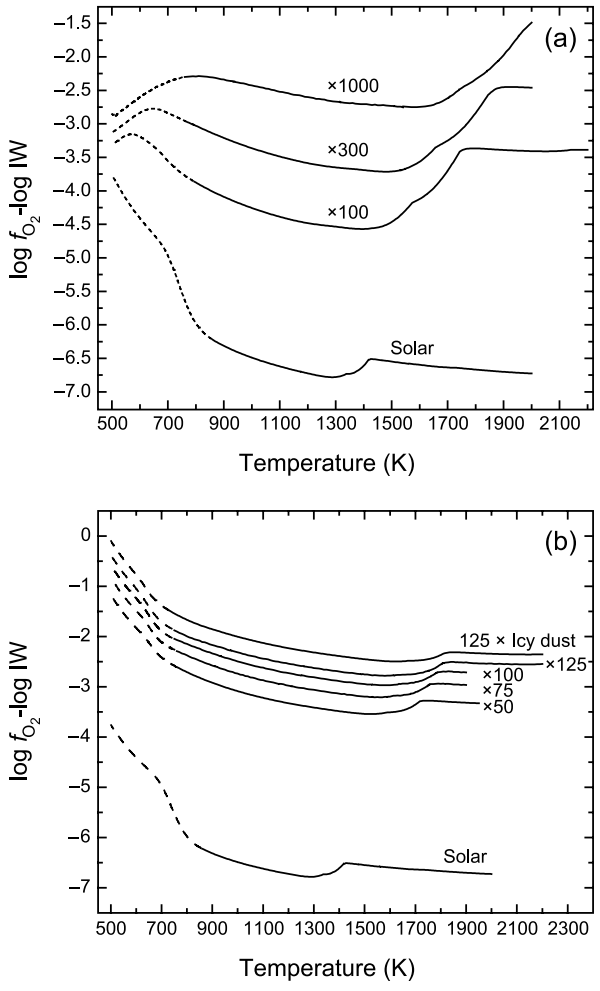

Fig. 3. Variation with temperature of the equilibrium $\log f_{O_2}$ relative to that of the iron-wüstite (IW) buffer at $P^{tot} = 10^{-3}$ bar in systems enriched in **(a)** OC dust by factors of 100, 300, and 10^3 and **(b)** C1 dust by factors of 50, 75, 100, and 125 or in icy dust (see text) by a factor of 125 relative to solar composition, in all cases compared to that of a system of solar composition. Each curve is dashed below the temperature at which the P_{CH_4}/P_{CO} ratio becomes ≥0.01, where the P_{H_2O}/P_{H_2} ratio becomes significantly affected by reaction (2).

slow. If the reaction were to occur homogeneously in the gas phase at ~800 K (*Lewis and Prinn,* 1980) or by catalysis on metallic Fe surfaces at ~600 K (*Prinn and Fegley*, 1989), for example, the $CO_{(g)}$ destruction time would be comparable to the solar nebular cooling time. Nevertheless, full equilibrium calculations were extended to 500 K in order to determine what the equilibrium state of the system actually is, for comparison with dust-enriched systems where reaction (2) becomes important only below the temperatures of interest in this work. The P_{H_2O}/P_{H_2} ratio is plotted in Fig. 2a, and the difference between the $\log f_{O_2}$ of solar gas and that of IW in Fig. 3a for the entire temperature range investigated here. The P_{H_2O}/P_{H_2} ratio is nearly constant at ~4.1×10^{-4} between 1800 K and 1400 K, falls to ~2.5×10^{-4} by 1300 K and remains constant until ~850 K. The decline that begins at ~1400 K is due to consumption of gaseous O by the major O-containing condensate, forsterite. Assuming equilibrium gas phase speciation, the P_{CH_4}/P_{CO} ratio is <0.01 above 850 K but begins to increase significantly below this temperature due to a shift to the right of reaction (2). Because of this, the P_{H_2O}/P_{H_2} ratio begins to rise below 850 K, reaching ~7.4×10^{-4} at 625 K where it remains until 500 K. Because reaction (2) is kinetically hindered, the solar gas curve in Fig. 2a is dashed below 850 K.

The difference between $\log f_{O_2}$ of solar gas and that of IW decreases slightly with falling temperature from 2000 to 1400 K, then increases slightly where the P_{H_2O}/P_{H_2} ratio drops due to olivine condensation. The difference begins to decrease gradually below 1300 K and then more steeply

below 850 K. Because the steep rise is due to the kinetically hindered reaction (2), the solar gas curve is again dashed below 850 K in Fig. 3a. It should be noted that, since wüstite is unstable below 843 K, the $\log f_{O_2}$ of solar gas is being compared to the metastable extension of the IW curve below this temperature. In summary, a gas of solar composition becomes progressively more capable of converting metallic Fe into oxidized Fe with decreasing temperature.

The effect of the temperature variation of $\log f_{O_2}$ on the equilibrium X_{Fa} in condensate olivine is shown in Fig. 4. In a solar gas, X_{Fa} is insignificant, and the olivine is virtually pure forsterite above 850 K. Below this temperature, where reaction (2) begins to contribute significantly to the P_{H_2O}/P_{H_2} ratio at equilibrium, the curve is dashed, indicating the kinetic inhibition of this reaction. Even if gas phase equilibrium were to persist below this temperature, allowing f_{O_2} to rise sharply, X_{Fa} would only reach 0.11 by 500 K. The increase in fayalite content is not due simply to an exchange of Fe^{2+} for Mg^{2+} in the existing olivine; rather, the total amount of olivine increases. This is because the source of Fe^{2+} is progressive oxidation of metallic Fe with falling temperature, creating a progressively greater (Mg + Fe^{2+})/Si ratio in the condensate. A source of Si is needed to consume the additional cations and, since the bulk of the Si not contained in olivine is predicted to be present as orthopyroxene in this temperature range, the latter must be converted into additional olivine. The reaction is written

$$2MgSiO_{3(c)} + 2Fe_{(c)} + 2H_2O_{(g)} \leftrightarrow Fe_2SiO_{4(c)} + Mg_2SiO_{4(c)} + 2H_{2(g)} \quad (3)$$

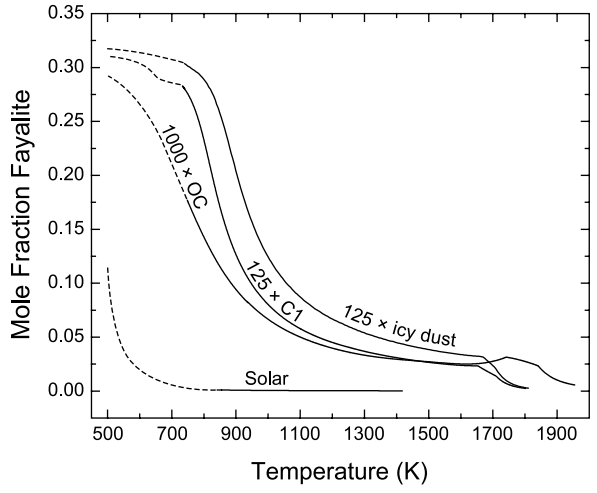

Fig. 4. Equilibrium fayalite content of condensate olivine as a function of temperature at a total pressure of 10^{-3} bar in a gas of solar composition and in cosmic gases enriched by a factor of 10^3 in OC dust, by a factor of 125 in dust of C1 chondrite composition, and by a factor of 125 in icy dust (see text). Each curve is dashed below the temperature at which the P_{CH_4}/P_{CO} ratio becomes ≥0.01, where the P_{H_2O}/P_{H_2} ratio becomes significantly affected by reaction (2).

At equilibrium, all olivine must have the same X_{Fa} at a given temperature, both the preexisting olivine and the newly created olivine. At 721 K, residual metallic Fe begins to react with $H_2S_{(g)}$ to form troilite, which consumes virtually all the sulfur and 48.6% of the Fe by 550 K. Because 37.1% of the total Fe remains in metallic form and is thus available for oxidation at 500 K, X_{Fa} is rising steeply when the calculation terminates at this temperature.

Reaction (3) is a solid-state reaction requiring the prior existence of enstatite, and controlled by the f_{O_2} of a coexisting fluid phase. Although reaction rate studies were used by *Imae et al.* (1993) to show that very little enstatite would be expected to form in the solar nebula, this phase has nevertheless been produced by *Toppani et al.* (2004) in 1-hr condensation experiments in high-temperature, low-pressure, multicomponent gases, and has been found by *Nguyen and Zinner* (2004) among presolar grains believed to have formed in stellar atmospheres in less than a few years. Equilibrium fayalite formation depends on a number of other factors, including equilibrium fluid phase speciation, intimate contact between reacting crystalline phases, high collision rates of gas species with the surfaces of these phases, and rapid solid-state diffusion (*Palme and Fegley,* 1990; *Krot et al.,* 2000). In this work, attention is focused on the degrees to which the sluggishness of gas phase reaction (2), the slow collision rate of Fe-bearing gaseous species with olivine crystal surfaces, and the slow rate of Fe-Mg interdiffusion in olivine at these temperatures affect the mean X_{Fa} of condensate olivine crystals.

Using equation (1), Fe-Mg interdiffusion coefficients were calculated from the f_{O_2}-temperature combinations along the solar gas curve in Fig. 3a. Using these, fayalite concentration profiles were calculated at successively lower temperatures until either a temperature was reached at which diffusion became so slow that further evolution of the profile was insignificant, or 850 K, where significant production of $H_2O_{(g)}$ via the kinetically hindered reaction (2) is required to occur at equilibrium, whichever was highest. Resulting concentration profiles for olivine crystals with radii of 3 μm and 1 μm immersed in a gas of solar composition during slow cooling are shown in Figs. 5a and 5b, respectively, and during fast cooling in Figs. 5c and 5d, respectively. In a solar gas at $P^{tot} = 10^{-3}$ bar, olivine first condenses at 1417 K with $X_{Fa} = 1.6 \times 10^{-4}$. The diffusion calculation for slow cooling begins at 1280 K, where the equilibrium X_{Fa} at the surface has risen to 2.8×10^{-4}. At this temperature, diffusion is fast enough that, for a 3-μm grain, the initial profile evolves into a uniform profile at $X_{Fa} = 3.0 \times 10^{-4}$ by 1250 K. Below 1100 K, however, the diffusion rate slows relative to the rate of increase of the surface concentration, and the profiles become steeply curved near the surface, as seen in Fig. 5a. By 850 K, the central X_{Fa} has reached 3.9×10^{-4} and the surface $X_{Fa} = 1.0 \times 10^{-3}$. At this point, the average X_{Fa} of the grain is 5.6×10^{-4}. When a 1-μm grain undergoes slow cooling, the concentration profile begins to curve below ~1050 K. By 850 K, the central $X_{Fa} = 4.6 \times 10^{-4}$, the surface $X_{Fa} = 1.0 \times$

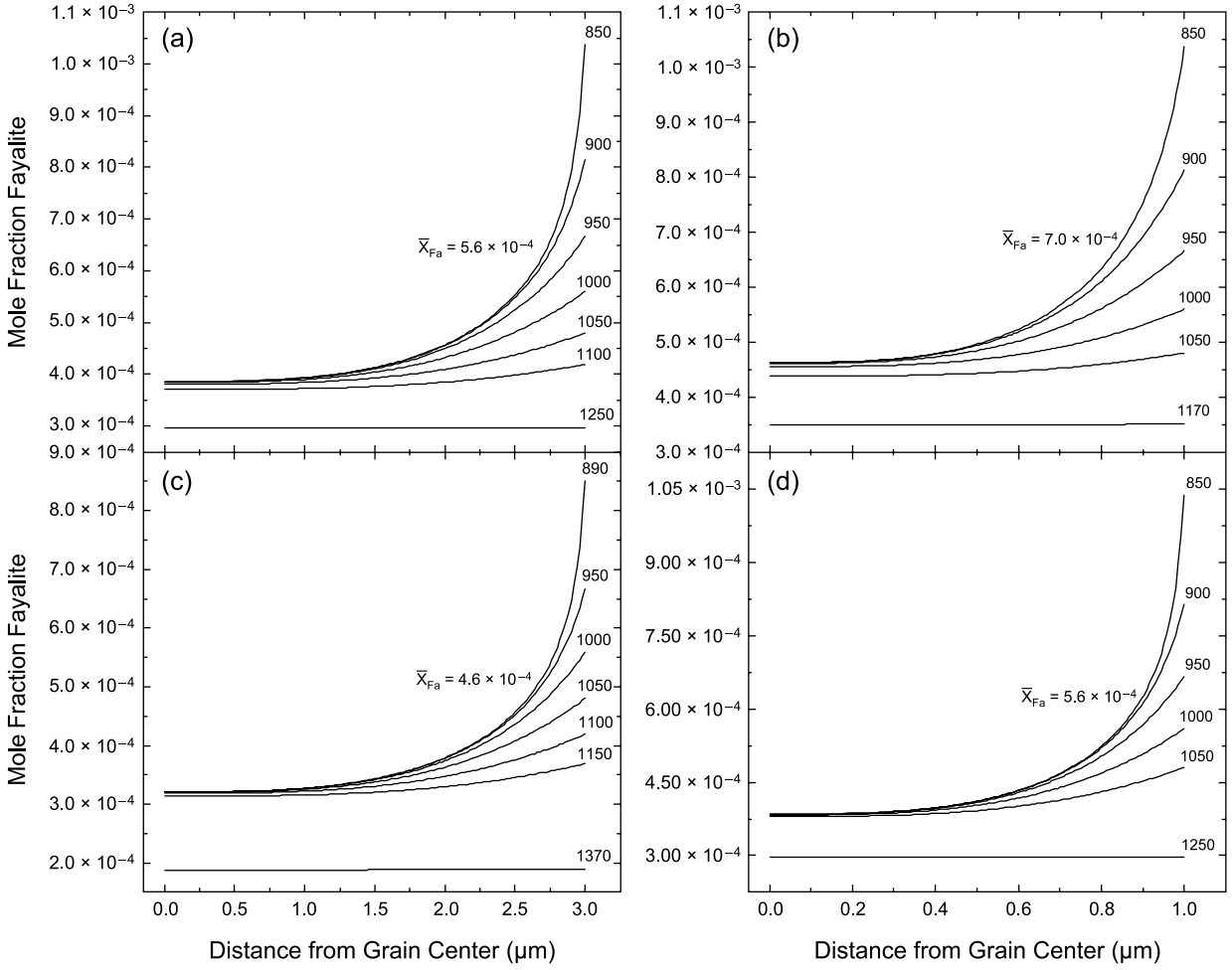

Fig. 5. Calculated variation of fayalite concentration with distance from the centers of condensate olivine crystals with radii of **(a,c)** 3 μm and **(b,d)** 1 μm whose surfaces are at equilibrium with the gas in a system of solar composition at $P^{tot} = 10^{-3}$ bar. For each grain size, profiles are shown at several temperatures during exponential cooling along the f_{O_2}-T path of a system of this composition, with decay constants of **(a,b)** 4.32×10^{-6} yr^{-1} and **(c,d)** 4.32×10^{-5} yr^{-1}. In each case, the numerical label associated with each curve is the temperature in Kelvins at which the profile was calculated, and the curve labeled with the mean X_{Fa} of the grain is the profile for the temperature below which diffusion becomes negligible.

10^{-3} and the mean $X_{Fa} = 7.0 \times 10^{-4}$ (Fig. 5b). In the case of fast cooling, the central X_{Fa} of a 3-μm grain has reached 3.2×10^{-4} at 890 K, and the surface $X_{Fa} = 8.5 \times 10^{-4}$ (Fig. 5c). At this point, the shapes of the profiles change very little with decreasing temperature except for the surface concentration, and the average X_{Fa} of the grain becomes virtually invariant with temperature, at a value of 4.6×10^{-4}. During fast cooling, the central $X_{Fa} = 4.0 \times 10^{-4}$, the surface $X_{Fa} = 1.0 \times 10^{-3}$, and the mean $X_{Fa} = 5.6 \times 10^{-4}$ for a 1-μm grain at 850 K (Fig. 5d).

The ability of olivine grains to reach their equilibrium X_{Fa} also depends on the rate of collision of gaseous Fe-containing species with olivine grain surfaces. In all cases considered in this work, the most abundant Fe-containing species is $Fe_{(g)}$ at high temperature and $Fe(OH)_{2(g)}$ at low temperature. At each temperature step of the condensation program, the partial pressure of the most abundant Fe-containing species was used to calculate the collision rate of gaseous Fe atoms with olivine grain surfaces. This was compared to the rate of change of the number of Fe atoms that must enter each olivine grain to produce the above diffusion profiles, calculated from the change in mean X_{Fa} for the same temperature step and olivine grain size. The collision rate is much higher than the entry rate at high temperature but falls very sharply with decreasing temperature, while the entry rate is relatively constant. The collision rate is assumed to be insufficient to support the entry rate at the temperature where the collision rate falls below 10× the entry rate. This temperature is well below the temperature at which the concentration profile becomes invariant, not only for each of the grain sizes and cooling rates considered above in a system of solar composition, but also

for all other cases considered in this work. Thus, the collision rate is not the limiting factor in establishing the mean X_{Fa} in all cases considered herein.

Having established that the mean X_{Fa} that can be reached by olivine grains in solar gas is so much lower than the minimum X_{Fa} of precursors of UOC chondrules, we now repeat the above calculations in various dust-enriched systems.

3.2. Enrichment in Ordinary Chondrite Dust

Yoneda and Grossman (1995) computed a dust composition, hereinafter abbreviated OC, closely approximating that of ordinary chondrites but with a solar S/Si ratio. Full equilibrium condensation calculations were performed over the temperature range 2000–500 K at $P^{tot} = 10^{-3}$ bar in a system enriched in OC dust by factors of 100, 300, and 10^3. The P_{H_2O}/P_{H_2} ratios in these systems are compared to that of a solar gas in Fig. 2a. In these systems, the equilibrium P_{CH_4}/P_{CO} ratio becomes >0.01 below 790, 770, and 750 K respectively. This indicates that the P_{H_2O}/P_{H_2} ratios are not significantly affected by reaction (2) above these temperatures. Because this reaction is kinetically hindered, the curves in Fig. 2a are dashed below these temperatures. As expected, the equilibrium P_{H_2O}/P_{H_2} ratios are much higher than in a gas of solar composition over almost all of the investigated temperature range, but they converge toward one another below 900 K and actually meet at 430 K, below the temperature range of this figure. This behavior is due to the fact that it is the dust whose composition is in equilibrium with the gas in a system of solar composition at 430 K, which is added to the gas in various proportions to yield the OC dust-enriched systems in this figure. All this dust must condense back out of each of the dust-enriched systems by 430 K, leaving the coexisting gas with the original P_{H_2O}/P_{H_2} ratio at this temperature. In other words, a gas of solar composition is saturated in OC dust at 430 K and, no matter how much of this dust is dissolved in the gas at higher temperature, all of it reaches its solubility limit when the system is cooled to that temperature, leaving the same gas composition behind in each case.

In the system enriched in OC dust by a factor of 10^3, the P_{H_2O}/P_{H_2} ratio is very high, ~0.18, at 2000 K, declines sharply with falling temperature to ~0.035 by ~1600 K due to condensation of large amounts of O in such major silicate phases as forsterite, remains approximately constant until ~1000 K, and then declines sharply again, this time due to oxidation of Fe according to reaction (3). The difference between $\log f_{O_2}$ in each of these systems and that of the IW buffer is plotted as a function of temperature in Fig. 3a, where it is compared to that of a solar gas. Below the temperature at which reaction (2) begins to contribute significantly to the P_{H_2O}/P_{H_2} ratio at equilibrium, these curves are dashed, indicating the kinetic inhibition of this reaction. The shapes of these curves largely parallel those of the P_{H_2O}/P_{H_2} ratios, but the important point is that all these systems are much more oxidizing than a gas of solar composition over almost all of the investigated temperature range. The f_{O_2} of a system enriched by a factor of 10^3 in OC dust relative to solar composition is 5 log units closer to IW and thus 5 log units more oxidizing at 2000 K, and more than 3 log units more oxidizing from 1700 K to 800 K, than a solar gas. In Fig. 4, the temperature variation of the equilibrium X_{Fa} of condensate olivine in this system is compared to that in a solar gas. At such large dust enrichments, condensation occurs at temperatures so high that silicate melt is stable and olivine forms above 1950 K. At equilibrium, its X_{Fa} is higher than in a solar gas over the entire temperature range, reaching 0.05 at ~1100 K, 0.25 at ~640 K, and 0.29 at 500 K. At 750 K, where reaction (2) begins to affect the P_{H_2O}/P_{H_2} ratio significantly, X_{Fa} has reached 0.18.

Fayalite zoning profiles in condensate olivine grains are shown in Fig. 6 for a system enriched in OC dust by a factor of 10^3. The curves in this figure are calculated as in Fig. 5, except that the Fe-Mg interdiffusion coefficients are computed from the f_{O_2}-temperature combinations along the curve labeled "×1000" in Fig. 3a instead of along the solar gas curve. The higher f_{O_2} at each temperature that is characteristic of this dust-enriched system leads to higher X_{Fa} at a given temperature, in accord with Fig. 4. Figure 6a shows that, during slow cooling in a system enriched in OC dust by a factor of 10^3 at $P^{tot} = 10^{-3}$ bar, the mean X_{Fa} of a 3-μm olivine grain becomes virtually invariant at 0.078 at 815 K, where its central $X_{Fa} = 0.054$ and its surface $X_{Fa} = 0.13$. The profile of a 1-μm grain becomes invariant at 780 K, where the mean $X_{Fa} = 0.093$ (Fig. 6b). During fast cooling, the 3-μm grain achieves a mean $X_{Fa} = 0.065$ before diffusion stops, and the 1-μm grain reaches $X_{Fa} = 0.078$. For each case considered, diffusion stops at a higher temperature than that where reaction (2) would begin to contribute significantly to the P_{H_2O}/P_{H_2} ratio at equilibrium, so these results are unaffected by the failure of this reaction to reach equilibrium. Because the predicted values for the mean X_{Fa} are below the minimum X_{Fa} of precursors of UOC chondrules, neither the fast- nor the slow-cooling condition is capable of producing condensate olivine grains with the desired properties in a system enriched in OC dust by a factor of 10^3, unless the grains are significantly smaller than 1 μm in radius.

On the other hand, the discrepancy between predicted and observed X_{Fa} is relatively small, suggesting that grains of the desired compositions could be produced at OC dust enrichments only slightly greater than 10^3. As can be seen in Fig. 3a, any gas composition enriched in OC dust by less than that amount will be less oxidizing, will yield lower X_{Fa} at each temperature, and will fall short of matching the minimum X_{Fa} of precursors of UOC chondrules by an amount that increases with decreasing dust enrichment factor. The problem with using enrichment in dust of this composition as an explanation of the minimum X_{Fa} of chondrule precursors of UOCs is that the necessary degree of dust enrichment, $>10^3$, is far beyond what seems possible from models of coagulation and settling in the solar nebula. *Cas-*

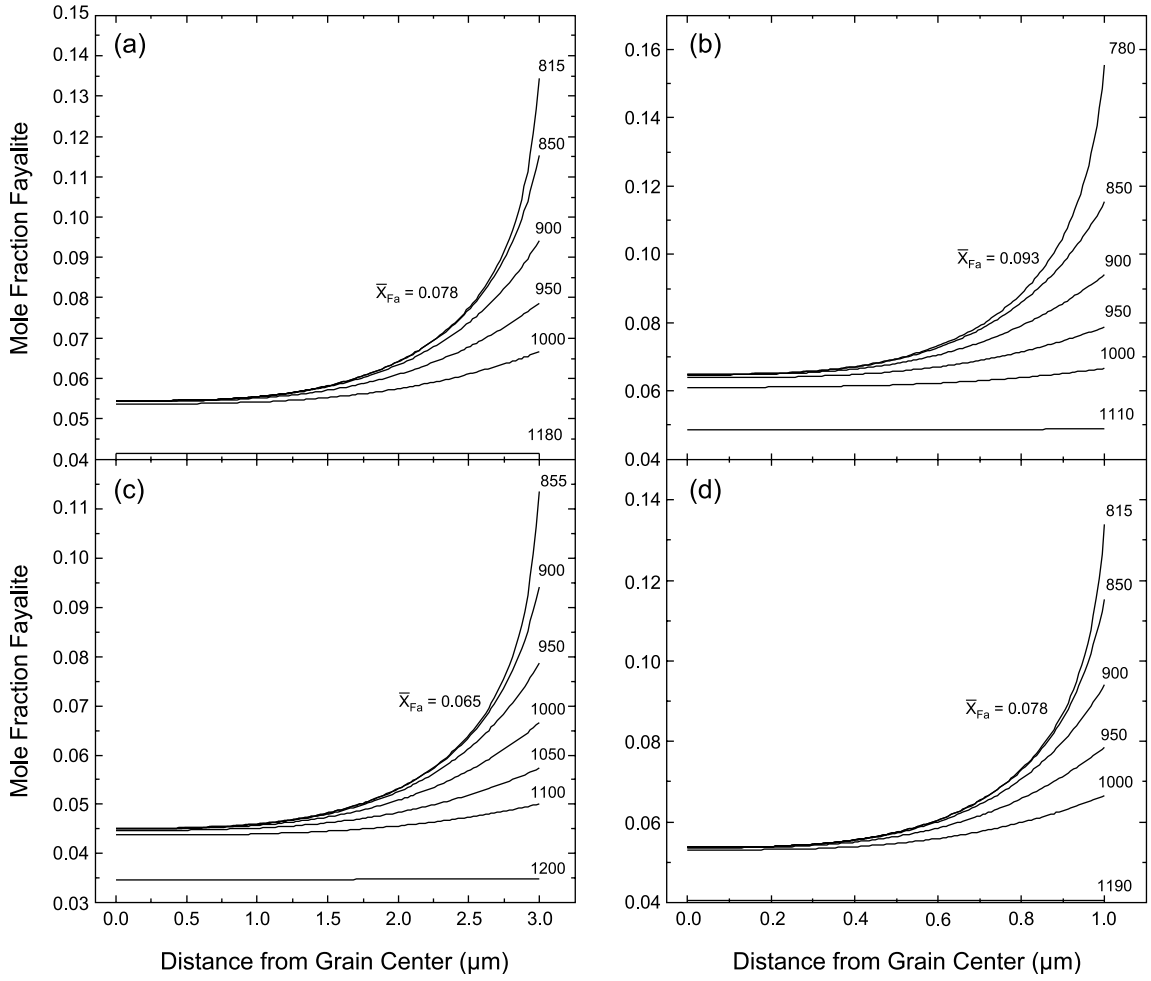

Fig. 6. Calculated variation of fayalite concentration with distance from the centers of condensate olivine crystals with radii of **(a,c)** 3 μm and **(b,d)** 1 μm whose surfaces are at equilibrium with the gas in a system enriched by a factor of 10^3 in OC dust at P^{tot} = 10^{-3} bar. For each grain size, profiles are shown at several temperatures during exponential cooling along the f_{O_2}-T path of a system of this composition, with decay constants of **(a,b)** 4.32×10^{-6} yr^{-1} and **(c,d)** 4.32×10^{-5} yr^{-1}. In each case, the numerical label associated with each curve is the temperature in Kelvins at which the profile was calculated, and the curve labeled with the mean X_{Fa} of the grain is the profile for the temperature below which diffusion becomes negligible.

sen (2001) showed that, while dust-enrichment factors of up to ~130 may be produced under some circumstances, much lower enrichments are more frequently encountered in such models. Thus, if the mean X_{Fa} of precursors of UOC chondrules was established by condensation in dust-enriched regions of the nebula, dust more O-rich than the OC composition must have been responsible in order for the necessary f_{O_2} to be produced at lower dust enrichments.

3.3. Enrichment in C1 Chondrite Dust

C1 chondrites have much higher H_2O, and therefore O, concentrations than ordinary chondrites. Full equilibrium condensation calculations were performed over the temperature range 1900–500 K at P^{tot} = 10^{-3} bar in systems enriched in C1 dust by factors of 50, 75, 100, and 125 relative to solar composition. The P_{H_2O}/P_{H_2} ratios in these systems are plotted as a function of temperature and compared to the ratios in a solar gas in Fig. 2b. In these systems, the equilibrium P_{CH_4}/P_{CO} ratio would become >0.01, and therefore reaction (2) would begin to affect the P_{H_2O}/P_{H_2} ratios significantly, below 760, 750, 740, and 740 K respectively. Because this reaction is kinetically hindered, the curves in Fig. 2b are dashed below these temperatures. The shapes of the curves for the C1 dust-enriched cases are very similar to that of solar gas but are displaced upward by 1–2 orders of magnitude relative to the latter. The P_{H_2O}/P_{H_2} ratios in the system enriched in C1 dust by a factor of 125 are quite comparable to those of the system enriched in OC dust by a factor of 10^3 over the temperature interval from 1600 to 900 K (Fig. 2a). Unlike the latter case, however, the equilibrium P_{H_2O}/P_{H_2} ratios in the system enriched in

C1 dust by a factor of 125 remain 50–120× higher than in a solar gas from 900 to 500 K. The differences between $\log f_{O_2}$ of the C1 dust-enriched systems and that of IW are plotted as a function of temperature in Fig. 3b, where they are compared to the same function for solar gas. In order to investigate the effect of P^{tot} on the f_{O_2} of a system enriched in C1 dust by a factor of 125, an identical condensation calculation was run in this system at $P^{tot} = 10^{-6}$ bar. Although not shown on Fig. 3b, the resulting curve for this system at $P^{tot} = 10^{-6}$ bar is coincident with that for the same dust enrichment at 10^{-3} bar below 1340 K. The shapes of the curves for the C1 dust-enriched cases are very similar to that of solar gas but are displaced upward by more than 3 orders of magnitude relative to the latter. Over the temperature range 1700 to 1000 K, $\log f_{O_2}$ of the system enriched in C1 dust by a factor of 125, ~IW-2.5, is very similar to that of the system enriched in OC dust by a factor of 10^3 (Fig. 3a). Below 1000 K, however, where the equilibrium $\log f_{O_2}$ of the system enriched in OC dust plunges with falling temperature to IW-2.8 by 500 K, that of the system enriched in C1 dust rises to ~IW-0.4 over the same temperature interval. The effect on X_{Fa} is shown in Fig. 4. From 1800 to 1000 K, the temperature interval where $\log f_{O_2}$ of the system enriched in C1 dust is similar to that of the system enriched in OC dust, X_{Fa} is also very similar in the two systems. Below 1000 K, however, the enhanced f_{O_2} of the system enriched in C1 dust causes X_{Fa} to rise more steeply with falling temperature than in the system enriched in OC dust, reaching 0.28 at ~740 K. Below this temperature, reaction (2) would begin to contribute significantly to the P_{H_2O}/P_{H_2} ratio if it were not kinetically inhibited. Even if equilibrium were maintained, however, the rate of increase of X_{Fa} with falling temperature would diminish, and X_{Fa} would level off at 0.31 at 500 K, as shown by the dashed extension of the curve labeled "125 × C1" in Fig. 4. For this enrichment, the curve of X_{Fa} vs. temperature for $P^{tot} = 10^{-6}$ bar is identical to the one shown at 10^{-3} bar below 1340 K.

In Fig. 7, fayalite zoning profiles in condensate olivine grains are shown at $P^{tot} = 10^{-3}$ bar in a system enriched in C1 dust by a factor of 125, a dust enrichment very close to the maximum found in *Cassen*'s (2001) coagulation and settling models. The curves in this figure are calculated as in Figs. 5 and 6, except that the Fe-Mg interdiffusion coefficients are computed from the f_{O_2}-temperature combinations along the curve labeled "×125" in Fig. 3b. The higher f_{O_2} of this system below 1000 K compared to the system enriched in OC dust by a factor of 10^3 results in higher values of the equilibrium X_{Fa} at each temperature, leading to higher average X_{Fa} in condensate olivine crystals. Figure 7a shows that, during slow cooling, the mean X_{Fa} of an olivine grain 3 μm in radius becomes virtually invariant at 0.11 at 790 K, where its central $X_{Fa} = 0.064$ and its surface $X_{Fa} = 0.24$. The profile of a grain whose radius is 1 μm becomes invariant at 770 K, where the mean $X_{Fa} = 0.14$. During fast cooling, the 3-μm grain achieves a mean $X_{Fa} = 0.08$ before diffusion stops, and the 1-μm grain reaches $X_{Fa} = 0.11$. For each case considered, diffusion stops at a temperature higher than 740 K, where reaction (2) begins to contribute significantly to the P_{H_2O}/P_{H_2} ratio at equilibrium, so these results are unaffected by the failure of reaction (2) to reach equilibrium. Because the temperature variations of both $\log f_{O_2}$ and X_{Fa} are identical at 10^{-3} bar and 10^{-6} bar in this temperature range, zoning profiles identical to those in Fig. 7 are obtained at a P^{tot} of 10^{-6} bar.

Thus, in a slowly cooled system enriched in C1 dust by a factor of 125 relative to solar composition, 3-μm olivine grains are produced whose average X_{Fa} is less than the minimum X_{Fa} of precursors of UOC chondrules. If faster cooling or larger grains are considered, the discrepancy between the calculated average X_{Fa} and the minimum value for UOC chondrule precursors becomes even greater. For grains with radii of 1 μm, the average X_{Fa} is very close to this value for slow cooling but not for fast cooling. Thus, in C1 dust-enriched systems, tiny olivine grains (radii ≤1 μm) can achieve an average X_{Fa} above the minimum X_{Fa} of precursors of UOC chondrules, but only at the highest dust enrichments and slowest cooling rates considered here. Only very tiny grains, with radii <~0.5 μm, can do so over the entire range of cooling rates considered here combined with the highest dust enrichments found in *Cassen*'s (2001) study. At much lower, but much more likely, dust enrichments, the average olivine condensate grain would have to be much smaller than 1 μm in order to reach the minimum X_{Fa}, 0.145. This cannot be considered a robust solution to the problem of how the Fe in the precursors of the chondrules of ordinary chondrites achieved its oxidation state.

Even if the precursor material of the UOCs did form at the highest dust enrichments and lowest cooling rates, the radius of the average olivine condensate grain would have to have been ≤1 μm in order to achieve the minimum X_{Fa} of this material. This small size does not seem reasonable. Isotopically anomalous single crystals of olivine and clinopyroxene, whose origin as condensates in the envelopes of AGB stars is indisputable, have radii up to 0.25 μm (*Nguyen and Zinner,* 2004). Because of the very high speed with which such grains escape AGB stars in stellar winds (*Bowen,* 1988), the observed grains must have grown in less than a few years (*Sharp and Wasserburg,* 1995). Combining the temperature interval over which $Mg_{(g)}$ is converted to forsterite in the systems considered in the present work with the solar nebular cooling times, the forsterite crystals into which the Fe must later diffuse grew over a period of at least several thousand years. While gas densities and supersaturation conditions must certainly differ between condensation in AGB stars and solar nebular condensation, it is unlikely that the typical size of a solar nebular condensate grain is less than that of a supernova condensate grain, and this seems to be borne out by observations in meteorites. It has been argued, for example, that fayalitic olivine laths in the matrix of Allende (*Wark,* 1979), hibonite crystals in the Murchison inclusion SH-6 (*MacPherson et al.,* 1984), "refractory" forsterite crystals in CM and CV chondrites (*Steele,* 1986; *Weinbruch et al.,* 2000), and radially zoned metal grains in CB chondrites (*Campbell et al.,* 2001) are primi-

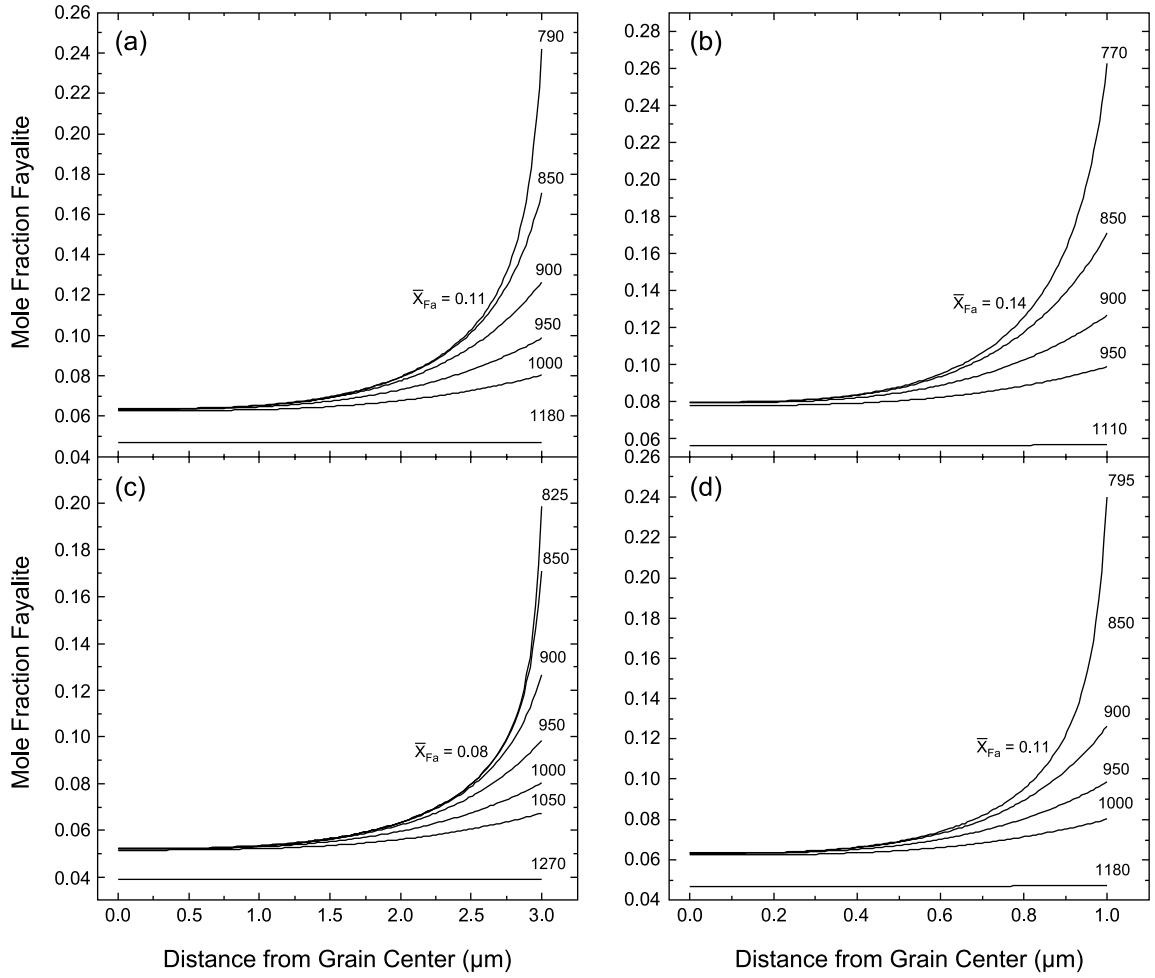

Fig. 7. Calculated variation of fayalite concentration with distance from the centers of condensate olivine crystals with radii of **(a,c)** 3 μm and **(b,d)** 1 μm whose surfaces are at equilibrium with the gas in a system enriched by a factor of 125 in dust of C1 chondrite composition at $P^{tot} = 10^{-3}$ bar. For each grain size, profiles are shown at several temperatures during exponential cooling along the f_{O_2}-T path of a system of this composition, with decay constants of **(a,b)** 4.32×10^{-6} yr^{-1} and **(c,d)** 4.32×10^{-5} yr^{-1}. In each case, the numerical label associated with each curve is the temperature in Kelvins at which the profile was calculated, and the curve labeled with the mean X_{Fa} of the grain is the profile for the temperature below which diffusion becomes negligible.

tive condensate grains from the solar nebula. While the hibonite crystals and fayalitic laths range from several micrometers up to 10 μm in length, the refractory forsterite and radially zoned metal grains can be up to several hundred micrometers in radius. Thus, the problem of the minimum X_{Fa} of olivine in precursors of UOC chondrules could be considered solved if a way could be found to produce olivine grains of at least several micrometers in radius whose mean $X_{Fa} \geq 0.145$.

3.4. Icy Dust with Higher Water Content than C1 Chondrites

A possible solution may be enrichment in dust that is even more O-rich than C1 chondrites. Suppose a type of nebular dust existed that contained solar proportions of condensable elements but was impregnated or coated with water ice such that the H_2O content exceeded that of C1 chondrites. Such icy dust is imagined to have been isolated from its complementary gas at a slightly lower temperature than C1 chondrites, such that more H_2O condensed into it, but no additional C. Total vaporization of a nebular region enriched in such dust would produce a system of higher f_{O_2} and stabilize higher fayalite contents at a given temperature than a system enriched by the same amount in C1 dust. For the purpose of investigating such a system, the primitive dust was assumed to have the composition of a mixture consisting of 1 part H_2O to 10 parts Orgueil by weight. Using the composition of Orgueil from *Anders and Grevesse* (1989), such dust would contain 25.5 wt% H_2O compared to 18.1% for Orgueil, and would have atomic O/Si and C/O ratios of 9.1 and 0.083, compared to 7.6 and 0.099 re-

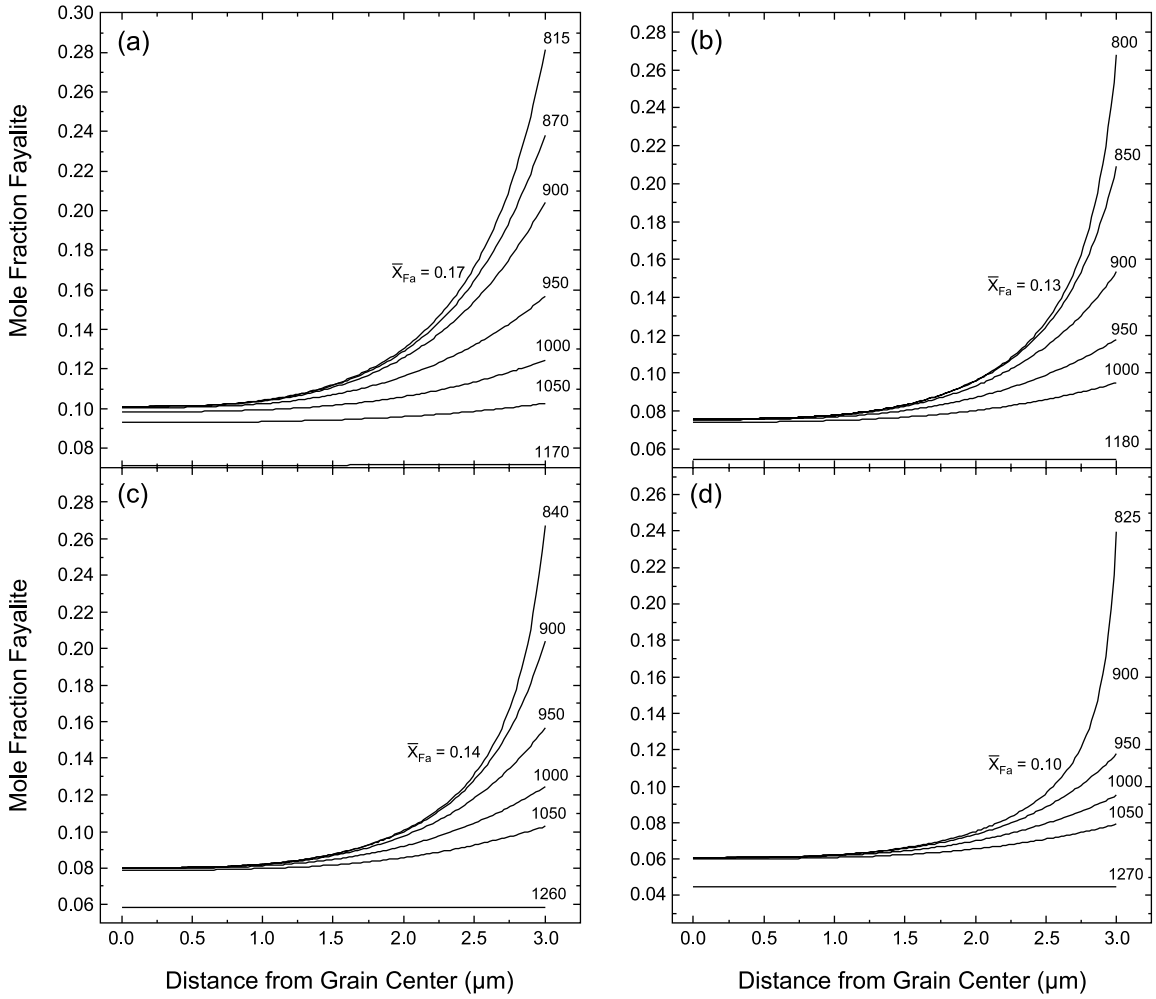

Fig. 8. Calculated variation of fayalite concentration with distance from the centers of condensate olivine crystals with radii of 3 μm whose surfaces are at equilibrium with the gas in a system enriched by a factor of **(a,c)** 125 and **(b,d)** 100 in icy dust (see text) at $P^{tot} = 10^{-3}$ bar. For each system composition, profiles are shown at several temperatures during exponential cooling along the appropriate f_{O_2}-T path, with decay constants of **(a,b)** 4.32×10^{-6} yr^{-1} and **(c,d)** 4.32×10^{-5} yr^{-1}. In each case, the numerical label associated with each curve is the temperature in Kelvins at which the profile was calculated, and the curve labeled with the mean X_{Fa} of the grain is the profile for the temperature below which diffusion becomes negligible.

spectively for Orgueil. Total condensation of such a region would produce material having chondritic relative proportions of nonvolatile elements.

The P_{H_2O}/P_{H_2} ratio of a system enriched in such icy dust by a factor of 125 relative to solar composition is plotted as a function of temperature, and compared to the ratios for systems enriched in C1 dust in Fig. 2b. In this system, reaction (2) would begin to contribute significantly to the P_{H_2O}/P_{H_2} ratio at 730 K if it were not kinetically inhibited. The shape of the curve for the icy dust-enriched system is very similar to that of the system enriched in C1 dust by a factor of 125 but is displaced upward by about 40% relative to the latter, below 1000 K. The difference between $\log f_{O_2}$ of the icy dust-enriched system and that of IW is plotted as a function of temperature in Fig. 3b, where it is compared to the same function for C1 dust-enriched systems. The shape of the curve for the icy dust-enriched system is very similar to that of the system enriched in C1 dust by a factor of 125 but is displaced upward by 0.3 log units relative to the latter, below 1000 K. The effect on X_{Fa} is shown in Fig. 4. The enhanced f_{O_2} of the system enriched in icy dust yields a higher X_{Fa} at each temperature than in the system enriched in C1 dust by a factor of 125. Critically important is the fact that X_{Fa} reaches 0.145 at 965 K in the icy dust-enriched system, compared to 875 K in the system enriched in C1 dust by a factor of 125.

In Figs. 8a and 8c, fayalite zoning profiles in condensate olivine grains are shown at $P^{tot} = 10^{-3}$ bar in a system enriched in icy dust by a factor of 125. The curves in this figure are calculated as in Figs. 5, 6, and 7, except that the Fe-Mg interdiffusion coefficients are computed from the f_{O_2}-temperature combinations along the curve labeled "125 ×

Icy dust" in Fig. 3b. The higher f_{O_2} of this system below 1000 K compared to the system enriched in C1 dust by a factor of 125 results in higher average X_{Fa} in condensate olivine crystals. Figure 8a shows that, during slow cooling in a system enriched in icy dust by a factor of 125, the mean X_{Fa} of an olivine grain 3 μm in radius becomes virtually invariant at 0.17 at 815 K, where its central $X_{Fa} = 0.10$ and its surface $X_{Fa} = 0.28$. During fast cooling, the grain achieves a mean $X_{Fa} = 0.14$ before diffusion stops. In a system enriched in icy dust by a factor of 100, f_{O_2} is ~0.1 log units higher than that for the system enriched in C1 dust by a factor of 125 at the same temperature. In such an icy dust-enriched system, the profile of a 3-μm grain becomes invariant at 800 K, where the mean $X_{Fa} = 0.13$, during slow cooling (Fig. 8b) and at 825 K, where the mean $X_{Fa} = 0.10$, during fast cooling (Fig. 8d). For each case considered, diffusion stops at a temperature higher than 730 K, where reaction (2) would begin to contribute significantly to the P_{H_2O}/P_{H_2} ratio at equilibrium, so these results are unaffected by the failure of reaction (2) to reach equilibrium.

Thus, in a system enriched in icy dust by a factor of 125 relative to solar composition, olivine grains with radii up to 3 μm will attain a mean X_{Fa} equal to or greater than the minimum X_{Fa} of precursors of UOC chondrules over the entire range of cooling rates investigated here. Even when the enrichment in icy dust is only a factor of 100 relative to solar composition, lower than the maximum found in coagulation and settling models, the mean X_{Fa} of 3-μm grains almost reaches the minimum needed for chondrule precursors at slow cooling but not at fast cooling. Thus, condensation of slowly cooled, icy dust-enriched regions could be considered a possible, minimal solution to the problem of how the mean X_{Fa} in chondrule precursors of primitive ordinary chondrites reached values of at least 0.145.

The opaque matrices of the least-equilibrated ordinary chondrites contain micrometer- to submicrometer-sized olivine grains whose average X_{Fa} ranges as high as 0.4 to 0.5, considerably greater than the mean X_{Fa} of the olivine in the chondrules in these meteorites, which is the focus of this study. While *Alexander et al.* (1989) argued that the fayalitic olivine in these matrices formed by parent-body metamorphism under relatively oxidizing conditions, *Huss et al.* (1981) suggested that this olivine could be a primitive condensate. If so, it is conceivable that such fayalite-rich material was the precursor of chondrules, and that olivine in the latter formed after reduction of this relatively FeO-rich material during chondrule formation. It should be emphasized, however, that no mechanism has been found in this study to produce, by equilibration with nebular gases, olivine of any grain size with such high fayalite contents. It was shown above that, at a given temperature, the equilibrium X_{Fa} of condensate olivine increases in systems with progressively higher f_{O_2}, and that, in each system, X_{Fa} reaches a maximum with falling temperature before leveling off. As seen in Fig. 4, however, these maxima on the equilibrium curves are only reached below the temperatures at which reaction (2) begins to affect the P_{H_2O}/P_{H_2} ratios significantly and, because this reaction does not proceed at equilibrium, these maximum values of X_{Fa} may not be reached. Furthermore, even if equilibrium were maintained, there is virtually no difference in the maximum X_{Fa} between the system enriched by a factor of 125 in icy dust and the one enriched by the same factor in C1 dust, despite the difference in f_{O_2} between the two systems. The reason for this behavior is shown in Figs. 9a and 9b, in which the equilibrium distribution of Fe between crystalline phases and vapor is compared in the two systems. In both systems, metallic Ni-Fe condenses at ~1710 K and begins to react with $H_2S_{(g)}$ to form troilite at ~1250 K. As the temperature falls in both systems, metallic Fe is gradually consumed to form fayalite and ferrosilite, but the higher f_{O_2} of the icy dust-enriched system causes the proportion of the total Fe in silicates to that in metal to increase more rapidly with falling temperature. This is the reason why the curve of X_{Fa} in Fig. 4 rises more steeply with falling temperature for the icy dust-enriched system than for the C1 dust-enriched system. Because the total S ultimately condenses as troi-

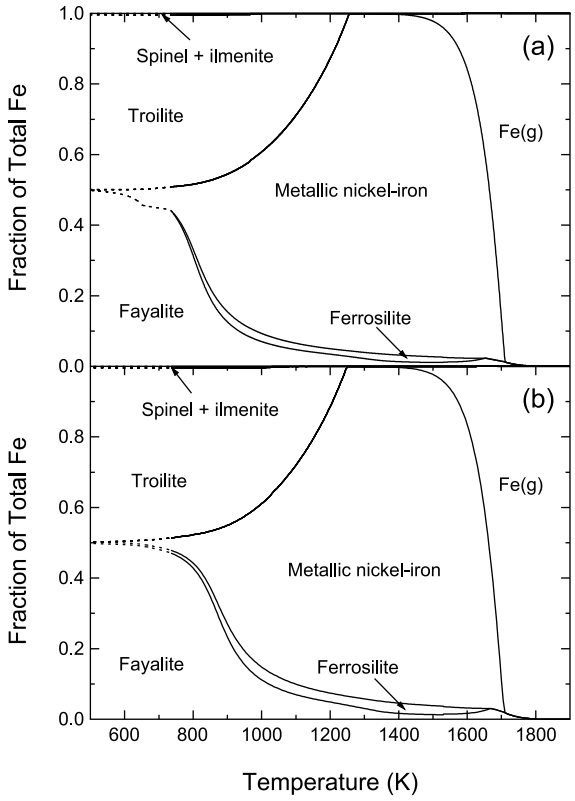

Fig. 9. Equilibrium distribution of Fe between crystalline phases and vapor as a function of temperature at $P^{tot} = 10^{-3}$ bar in a system enriched by a factor of 125 in **(a)** dust of C1 chondrite composition and **(b)** icy dust. Each curve is dashed below the temperature at which the P_{CH_4}/P_{CO} ratio becomes ≥0.01, where the P_{H_2O}/P_{H_2} ratio becomes significantly affected by reaction (2). Despite the higher f_{O_2} in **(b)**, the maximum fraction of the total Fe in silicates is the same.

lite, thereby consuming 49.6% of the total Fe in both systems, however, the fraction of the total Fe that forms fayalite can never exceed 50.4%, corresponding to $X_{Fa} = 0.32$, regardless of the difference between the two systems in f_{O_2} or in the rate of increase of the proportion of Fe in silicates with temperature. This value is much lower than the range of X_{Fa} seen in the matrices of UOCs.

The minimum dust enrichment required to produce condensate olivine grains with radii ≥1 μm and mean X_{Fa} above the desired value over the entire range of nebular midplane cooling rates lies within the range of dust enrichments encountered in astrophysical models of coagulation and settling only if the dust is more O-rich than C1 chondrites. Such conditions by themselves, however, are insufficient to yield at least one other fundamental mineralogical characteristic of ordinary chondrites: the distribution of Fe among coexisting metallic, sulfide, and silicate phases. In the above models, a maximum temperature is found at which the mean X_{Fa} of zoned condensate olivine grains is frozen in at the minimum X_{Fa} of the precursors of UOC chondrules. In the system enriched in icy dust by a factor of 125, this temperature ranges from 815 to 840 K for 3-μm grains, depending on cooling rate. In this temperature range, ~94% of the sulfur will have condensed, causing ~47% of the Fe to be in troilite, ~41% in silicates, and only ~12% in metallic Ni-Fe, as seen in Fig. 9b. All ordinary chondrites are depleted in S relative to Si by ~75% compared to solar abundances, presumably because metallic Ni-Fe grains were isolated from further reaction with the gas at a temperature above that necessary for complete condensation of S, due either to their being armored or buried during accretion. As a result, only 12.6%, 16.7%, and 18.7% of the total Fe in H, L, and LL chondrites, respectively, occurs as troilite (*Jarosewich,* 1990), much lower than would be expected had equilibrium conversion of metallic Fe to troilite continued to the same temperature as that where the minimum X_{Fa} of the precursors of chondrules in these meteorites was established by oxidation of the same metallic Fe grains. For condensate grains with mean X_{Fa} greater than the minimum value, the discrepancy between the cessation temperature of oxidation of the metal grains and that of sulfidation of the same population of grains would be even greater. This is an important drawback of using any dust containing solar proportions of condensable elements to enhance the f_{O_2} of the nebular source of the ordinary chondrites. A possible solution is to enrich a nebular region in dust that is even more ice-rich than that used above. This would lower the magnitude of the dust enrichment required to produce a mean $X_{Fa} = 0.145$ at 850 K. Although the lower dust enrichment would, in turn, lower the condensation temperature of troilite, the effect would probably be insufficient to prevent 75% of the S from condensing by 850 K.

3.5. Limitations

As seen above, computation of the mean X_{Fa} of an olivine grain of a given size is based on a diffusion calculation. In all the experimental determinations of interdiffusion rates in olivine reviewed above, the Fe-Mg interdiffusion coefficients, Ds, have similar temperature- and f_{O_2}-dependences as those in equation (1), but the lowest temperature at which any of those measurements was made is 1173 K, and the lowest f_{O_2} ~10^{-13}. In this work, extrapolation of these data to ~800 K and f_{O_2} ~10^{-30} assumes no change in diffusion mechanism in the intervening intervals of temperature and f_{O_2} that would alter these dependences. Although D is known to be anisotropic in olivine, and olivine crystals exhibit a variety of aspect ratios, the calculations in this work were simplified by assuming spherical geometry and isotropic diffusion, and by employing Ds parallel to the c-axis. The error introduced by doing so is limited, however, as Ds parallel to the different crystallographic axes vary by only a factor of ~3. This is relatively small compared to the difference between the Ds of *Chakraborty* (1997), which are employed in this study, and those of *Nakamura and Schmalzried* (1984), which are a factor of 10 higher at 1323 K. When the latter data are used in the case of enrichment in icy dust by a factor of 125, the 3-μm grains reach $X_{Fa} = 0.19$ and 0.16 during slow and fast cooling, respectively, instead of 0.17 and 0.14, which were estimated above. The differences in mean X_{Fa} produced by substituting the *Nakamura and Schmalzried* (1984) data for the *Chakraborty* (1997) data are thus so small that our conclusions about icy dust-enriched systems would be little affected. Correcting for diffusion anisotropy is expected to produce even smaller differences.

The diffusion calculations in this work require the results of condensation calculations as input parameters. Although the condensation calculations assume complete equilibrium, requiring that all grains of solid solution minerals be uniform and homogeneous in composition, the diffusion calculation shows that condensate olivine grains will, in reality, be zoned in composition. Thus, a possible limitation of the results presented here is that the effect of olivine zonation has not been fed back into the condensation calculation. This effect is expected to be minor in the dust-enriched systems, as it results in more excess metallic Fe and only slightly higher P_{H_2O}/P_{H_2} ratios than in the equilibrium cases calculated here. Another possible limitation is that negligible olivine grain growth is assumed to occur as its concentration changes.

4. CONCLUSIONS

A gas of solar composition is too reducing to allow the equilibrium X_{Fa} in condensate olivine to reach the minimum X_{Fa} of the precursors of UOC chondrules, 0.145, at temperatures above that where gas phase equilibrium breaks down or where Fe-Mg interdiffusion in olivine stops. When a region enriched in dust relative to gas compared to solar composition is vaporized, the resulting vapor has higher f_{O_2} than a gas of solar composition. In such dust-enriched systems, the equilibrium X_{Fa} of olivine at almost any temperature is higher than in a system of solar composition, and the amount by which it is increased increases with the degree of dust enrichment. For OC dust, even enrichments of

10^3 relative to solar composition are insufficient to produce a mean X_{Fa} in condensate olivine crystals with radii of 1 μm and 3 μm that is above the desired level at temperatures where diffusion occurs. Only dust-enrichment factors near the maximum allowed in coagulation and settling models, together with C1 chondrite dust whose O content has been enhanced by admixture of water ice, can yield olivine condensate grains with radii ≥1 μm whose mean X_{Fa} exceeds the minimum X_{Fa} of the precursors of UOC chondrules over the entire range of nebular midplane cooling rates. This unlikely set of circumstances cannot be considered a robust solution to the problem of the relatively high fayalite content of UOC olivine, which remains unsolved.

Acknowledgments. We are grateful for valuable advice from A. J. Campbell and J. Ganguly on diffusion calculations, and from M. Ghiorso on treatment of non-ideality in olivine and orthopyroxene. We thank T. Bernatowicz, J. N. Grossman, G. R. Huss, R. Jones, V. Kress, S. B. Simon, and S. Yoneda for helpful discussions. The manuscript benefited from the in-depth comments of three anonymous reviewers. This research was supported by funds from the National Aeronautics and Space Administration through grant NAG5-11588.

REFERENCES

Alexander C. M. O., Hutchison R., and Barber D. J. (1989) Origin of chondrule rims and interchondrule matrices in unequilibrated ordinary chondrites. *Earth Planet. Sci. Lett., 95,* 187–207.

Allende Prieto C., Lambert D. L., and Asplund M. (2001) The *forbidden* abundance of oxygen in the sun. *Astrophys. J. Lett., 556,* L63–L66.

Allende Prieto C., Lambert D. L., and Asplund M. (2002) A reappraisal of the solar photospheric C/O ratio. *Astrophys. J. Lett., 573,* L137–L140.

Anders E. and Grevesse N. (1989) Abundances of the elements: Meteoritic and solar. *Geochim. Cosmochim. Acta, 53,* 197–214.

Beckett J. R. (1986) The origin of calcium-, aluminum-rich inclusions from carbonaceous chondrites: An experimental study. Ph.D. thesis, University of Chicago.

Berman R. G. (1988) Internally-consistent thermodynamic data for minerals in the system Na_2O-K_2O-CaO-MgO-FeO-Fe_2O_3-Al_2O_3-SiO_2-TiO_2-H_2O-CO_2. *J. Petrol., 29,* 445–522.

Bowen G. H. (1988) Dynamical modeling of long-period variable star atmospheres. *Astrophys. J., 329,* 299–317.

Brearley A. J. and Jones R. H. (1998) Chondritic meteorites. In *Planetary Materials* (J. J. Papike, ed.), pp. 3-1 to 3-398. Reviews in Mineralogy, Vol. 36, Mineralogical Society of America.

Buening D. K. and Buseck P. R. (1973) Fe-Mg lattice diffusion in olivine. *J. Geophys. Res., 78,* 6852–6862.

Campbell A. J., Humayun M., Meibom A., Krot A. N., and Keil K. (2001) Origin of metal grains in the QUE94411 chondrite. *Geochim. Cosmochim. Acta, 65,* 163–180.

Cassen P. (2001) Nebular thermal evolution and the properties of primitive planetary materials. *Meteoritics & Planet. Sci., 36,* 671–700.

Chakraborty S. (1997) Rates and mechanisms of Fe-Mg interdiffusion in olivine at 980°–1300°C. *J. Geophys. Res., 102,* 12317–12331.

Chase M. W. Jr., Davies C. A., Downey J. R., Frurip D. J., McDonald R. A., and Syverud A. N. (1985) *JANAF Thermochemical Tables, 3rd edition. J. Phys. Chem. Ref. Data, 14, Suppl. 1.* Dow Chemical Company, Midland, Michigan.

Crank J. (1975) *The Mathematics of Diffusion, 2nd edition*. Oxford Univ., Oxford.

Dodd R. T. Jr., Van Schmus W. R., and Koffman D. M. (1967) A survey of the unequilibrated ordinary chondrites. *Geochim. Cosmochim. Acta, 31,* 921–951.

Dohmen R., Chakraborty S., Palme H., and Ramensee W. (1998) Solid-solid reactions mediated by a gas phase: An experimental study of reaction progress and the role of surfaces in the system olivine + iron metal. *Am. Mineral., 83,* 970–984.

Dowty E. and Clark J. R. (1973) Crystal structure refinement and optical properties of a Ti^{3+} fassaite from the Allende meteorite. *Am. Mineral., 58,* 230–242.

Ebel D. S. and Grossman L. (2000) Condensation in dust-enriched systems. *Geochim. Cosmochim. Acta, 64,* 339–366.

Fedkin A. V. and Grossman L. (2004) Nebular formation of fayalitic olivine: Ineffectiveness of dust enrichment (abstract). In *Lunar and Planetary Science XXXV,* Abstract #1823. Lunar and Planetary Institute, Houston (CD-ROM).

Gronvold F. and Stolen S. (1992) Thermodynamics of iron sulfides II. Heat capacity and thermodynamic properties of FeS and of $Fe_{0.875}S$ at temperatures from 298.15K to 1000K, of $Fe_{0.98}S$ from 298.15K to 800K, and of $Fe_{0.89}S$ from 298.15K to about 650K. Thermodynamics of formation. *J. Chem. Thermodyn., 24,* 913–936.

Grossman L. (1972) Condensation in the primitive solar nebula. *Geochim. Cosmochim. Acta, 36,* 597–619.

Grossman L. (1980) Refractory inclusions in the Allende meteorite. *Annu. Rev. Earth Planet. Sci., 8,* 559–608.

Grossman L., Ebel D. S., Simon S. B., Davis A. M., Richter F. M., and Parsad N. M. (2000) Major element chemical and isotopic compositions of refractory inclusions in C3 chondrites: The separate roles of condensation and evaporation. *Geochim. Cosmochim. Acta, 64,* 2879–2894.

Grossman L., Ebel D. S., and Simon S. B. (2002) Formation of refractory inclusions by evaporation of condensate precursors. *Geochim. Cosmochim. Acta, 66,* 145–161.

Grossman L. and Fedkin A. V. (2003) Nebular oxidation of iron (abstract). *Geochim. Cosmochim. Acta, 67, Suppl.,* A125.

Huss G. R., Keil K., and Taylor G. J. (1981) The matrices of unequilibrated ordinary chondrites: Implications for the origin and history of chondrites. *Geochim. Cosmochim. Acta, 45,* 33–51.

Imae N., Tsuchiyama A., and Kitamura M. (1993) An experimental study of enstatite formation reaction between forsterite and Si-rich gas. *Earth Planet. Sci. Lett., 118,* 21–30.

Jarosewich E. (1990) Chemical analyses of meteorites: A compilation of stony and iron meteorite analyses. *Meteoritics, 25,* 323–337.

Krot A. N., Fegley B. Jr., Lodders K., and Palme H. (2000) Meteoritical and astrophysical constraints on the oxidation state of the solar nebula. In *Protostars and Planets IV* (V. Mannings et al., eds.), pp. 1019–1054. Univ. of Arizona, Tucson.

Larimer J. W. (1975) The effect of C/O ratio on the condensation of planetary material. *Geochim. Cosmochim. Acta, 39,* 389–392.

Lewis J. S. and Prinn R. G. (1980) Kinetic inhibition of CO and N_2 reduction in the solar nebula. *Astrophys. J., 238,* 357–364.

Lodders K. (2003) Solar system abundances and condensation temperatures of the elements. *Astrophys. J., 591,* 1220–1247.

MacPherson G. J., Bar-Matthews M., Tanaka T., Olsen E., and Grossman L. (1983) Refractory inclusions in the Murchison meteorite. *Geochim. Cosmochim. Acta, 47,* 823–839.

MacPherson G. J., Grossman L., Hashimoto A., Bar-Matthews M., and Tanaka T. (1984) Petrographic studies of refractory inclusions from the Murchison meteorite. In *Proc. Lunar Planet. Sci. Conf. 15th,* in *J. Geophys. Res., 89,* C299–C312.

McCoy T. J., Scott E. R. D., Jones R. H., Keil K., and Taylor G. J. (1991) Composition of chondrule silicates in LL3–5 chondrites and implications for their nebular history and parent body metamorphism. *Geochim. Cosmochim. Acta, 55,* 601–619.

Misener D. J. (1974) Cationic diffusion in olivine to 1400°C and 35 kbar. In *Geochemical Transport and Kinetics* (A. W. Hofmann et al., eds.), pp. 117–129. Carnegie Institution of Washington Publication 634, Washington, DC.

Miyamoto M., Mikouchi T., and Arai T. (2002) Comparison of Fe-Mg interdiffusion coefficients in olivine. *Antarct. Meteorite Res., 15*, 143–151. National Institute of Polar Research, Tokyo.

Nakamura A. and Schmalzried H. (1984) On the Fe^{2+}-Mg^{2+} interdiffusion in olivine (II). *Ber. Bunsenges. Phys. Chem., 88,* 140–145.

Nguyen A. N. and Zinner E. (2004) Discovery of ancient silicate stardust in a meteorite. *Science, 303,* 1496–1499.

Palme H. and Fegley B. Jr. (1990) High-temperature condensation of iron-rich olivine in the solar nebula. *Earth Planet. Sci. Lett., 101,* 180–195.

Prinn R. G. and Fegley B. Jr. (1989) Solar nebula chemistry: Origin of planetary, satellite, and cometary volatiles. In *Origin and Evolution of Planetary and Satellite Atmospheres* (S. K. Atreya et al., eds.), pp. 78–136. Univ. of Arizona, Tucson.

Rambaldi E. R. (1981) Relict grains in chondrules. *Nature, 293,* 558–561.

Rietmeijer F. J. M. (1998) Interplanetary dust particles. In *Planetary Materials* (J. J. Papike, ed.), pp. 2-1 to 2-95. Reviews in Mineralogy, Vol. 36, Mineralogical Society of America.

Robie R. A., Hemingway B. S., and Fisher J. R. (1978) *Thermodynamic Properties of Minerals and Related Substances at 298.15K and 1 Bar (10^3 Pascals) Pressure and at Higher Temperatures.* U.S. Geological Survey Bulletin No. 1452.

Robinson G. R. Jr., Haas J. L. Jr., Schafer C. M., and Haselton H. T. Jr. (1982) *Thermodynamic and Thermophysical Properties of Selected Phases in the MgO-SiO_2-H_2O-CO_2, CaO-Al_2O_3-SiO_2-H_2O-CO_2, and Fe-FeO-Fe_2O_3-SiO_2 Chemical Systems, with Special Emphasis on the Properties of Basalts and Their Mineral Components.* U.S. Geological Survey Open-File Report No. 83-79.

Sack R. O. and Ghiorso M. S. (1989) Importance of considerations of mixing properties in establishing an internally consistent thermodynamic database: Thermochemistry of minerals in the system Mg_2SiO_4-Fe_2SiO_4-SiO_2. *Contrib. Mineral. Petrol., 102,* 41–68.

Sharp C. M. and Wasserburg G. J. (1995) Molecular equilibria and condensation temperatures in carbon-rich gases. *Geochim. Cosmochim. Acta, 59,* 1633–1652.

Steele I. M. (1986) Compositions and textures of relic forsterite in carbonaceous and unequilibrated ordinary chondrites. *Geochim. Cosmochim. Acta, 50,* 1379–1395.

Toppani A., Libourel G., Robert F., Ghanbaja J., and Zimmermann L. (2004) Synthesis of refractory minerals by high-temperature condensation of a gas of solar composition (abstract). In *Lunar and Planetary Science XXXV,* Abstract #1726. Lunar and Planetary Institute, Houston (CD-ROM).

Tscharnuter W. M. and Boss A. P. (1993) Formation of the protosolar nebula. In *Protostars and Planets III* (E. H. Levy and J. I. Lunine, eds.), pp. 921–938. Univ. of Arizona, Tucson.

Wark D. A. (1979) Birth of the presolar nebula: The sequence of condensation revealed in the Allende meteorite. *Astrophys. Space Sci., 65,* 275–295.

Weinbruch S., Palme H., and Spettel B. (2000) Refractory forsterite in primitive meteorites: Condensates from the solar nebula? *Meteoritics & Planet. Sci., 35,* 161–171.

Wood J. A. (1967) Olivine and pyroxene compositions in Type II carbonaceous chondrites. *Geochim. Cosmochim. Acta, 31,* 2095–2108.

Yoneda S. and Grossman L. (1995) Condensation of CaO-MgO-Al_2O_3-SiO_2 liquids from cosmic gases. *Geochim. Cosmochim. Acta, 59,* 3413–3444.